21, rue d'Artois, F-75008 PARIS
http : //www.cigre.org

CIGRE US National Committee
2016 Grid of the Future Symposium

Prediction of System Frequency Excursions for Centralized Load Shedding Applications

E.A. MOHAMED, M.S. ZEYADA, A.A. KARRAR, A.H. ELTOM

University of Tennessee at Chattanooga
USA

abdelrahman-karrar@utc.edu

SUMMARY

In this study centrally collected real-time frequency data from PMUs was used to build an estimate of the maximum frequency excursions in the event of a large generation outage or islanding conditions. The data is processed to perform corrections to the centre-of-inertia rate of change of frequency, which contains information not contributing to collective system dynamics. The objective is to remove the inter-generator oscillatory behaviour and control system dynamics, and retain only collective system behaviour reminiscent of lumped networks. Two methods are presented for correction; smoothing the rate of change of frequency using an averaging process, and correction of the disturbance power by removing initial oscillatory components. Curve fitting of the processed data to an exponentially damped sinusoid model is then performed to obtain a trend and predict the expected frequency excursions. The predicted frequency dips and time to minimum frequency would then serve as valuable information to support the automated real-time decision to withhold load shedding of the customers if the frequency is predicted to recover without violation of an enforced reliability criteria, for example the PRC-006-1 of NERC. A number of case studies were simulated on the IEEE 39 bus system model using real-time computation and hardware in the loop involving PMU's and a Synchro-phasor vector processor (SVP). The studies demonstrated that the method was successful in predicting the minimum frequency excursions provided a sufficient prediction interval was achievable.

KEYWORDS

Under-frequency load shedding (UFLS), disturbance power, real-time digital simulator, Phasor measurement units (PMUs), Synchro-phasor vector processor (SVP).

I. INTRODUCTION

Adaptive frequency load shedding schemes based on centralized processing of PMU measurements offer the potential for correctly estimating the amount of disturbance power to be shed and determining optimum locations for performing the shedding upon encountering islanding conditions [1]. The first step of load shedding is set by some utilities to 59.5 Hz, and it is generally accepted that the absolute minimum to avoid damage to steam turbines should be about 57 Hz [2]. However the Northern American Electric Reliability Corporation (NERC) standard PRC-006-1 for Automatic Under-frequency Load Shedding [3] defines in requirement R3-3.1 that: " Frequency shall remain above the Under-frequency Performance Characteristic curve in PRC-006-1 - Attachment 1, either for 60 seconds or until a steady-state condition between 59.3 Hz and 60.7 Hz is reached". It is inferred from the curve enclosed in the standard as an attachment that system frequency should never venture below 58 Hz and may remain above 58.8 for 60 seconds. After 60 seconds it must be restored to above 59.3 Hz.

Load shedding based on local frequency measurements is not satisfactory; being prone to shed too much or too little due to inter-generator and control system dynamics, and a centralized approach is considered more representative of the disturbance power [4]. However the centrally calculated disturbance power is not a fixed amount and varies with time as the generators swing against each other and as the generator excitation and prime movers respond to regulate voltage and frequency, thereby influencing the respective sensitive load components. If, however, despite these anomalies a reasonable estimate of collective system frequency behavior could be coerced from the system then the information could be used to predict the ensuing frequency behavior. It may well be the case that the system frequency, on account of sufficient spinning reserve and fast governor action, will reverse its downward frequency trend and recover with no shedding action or with a minimal amount of shedding. The key to predicting this behavior is to monitor the collective rate of change of system frequency and to observe changes in its slope which if consistent will lead to the reversal of the behavior of the collective frequency itself.

In this study islanding conditions were simulated on the IEEE 39 bus system [5] and the resulting frequency and rate of change of frequency responses were analyzed in real time in an attempt to predict the frequency trend and to use that prediction to influence load shedding decisions

II. DYNAMICS OF LUMPED VS. ACTUAL SYSTEMS

It is explained here how the actual behavior of the island system frequency differs from that of its approximate lumped representation in the event of a sudden power deficit resulting from island conditions.

A. Linear lumped model of a power system

It is possible to approximate the frequency behavior of an islanded power system with a linear frequency response behavior which depends on basic factors governing the response [2]. Other attempts to use low order frequency systems models are found in [4] and [6]. The factors influencing the frequency are the system inertia H, system damping D, generator droop regulation R (or alternatively, the gain K_m) and two parameters associated with boiler response F_R and T_R. The resulting system frequency excursion of the lumped model under islanded condition can be shown to have the general form of the exponentially damped sinusoid in (1)

$$\Delta f(t) = \alpha\left[1 + \beta e^{-\zeta\omega_n \cdot t}\sin(\omega_d t + \phi)\right] \qquad (1) \qquad \text{Where } \omega_d = \sqrt{1-\zeta^2}\cdot\omega_n$$

The frequency-time response evaluated from the model in response to a sudden load deficit brought upon by an islanding event will follow the behavior of a damped sinusoid as shown in Fig. 1. Outaged generation is 0.6 p.u and system parameters are defined in [2].

B. Actual System Dynamics and COI frequency oscillation

Fig. 2 shows frequency excursions on the IEEE 39 bus system upon an outage of Generator 2, which was dropped for the purposes of creating a power deficit in the system. The resulting frequency excursions of the remaining individual 9 units are shown in Fig. 2. The center of inertia (COI) frequency is also shown on the plot. It is customary to assume that the COI frequency is representative of the overall dynamics of the system and could be reasonably approximated by lumped system behavior [7]. However in reality the COI frequency does not exactly follow the lumped linear behavior, particularly during the first few moments following the disturbance because its derivative – the COI df/dt - oscillates around some central value. The COI df/dt oscillation was accurately described in [7] and is caused by system conductance losses during inter-generator oscillations. An additional influence is the initial voltage changes caused the redistribution of reactive power following the outage and the subsequent generator excitation response.

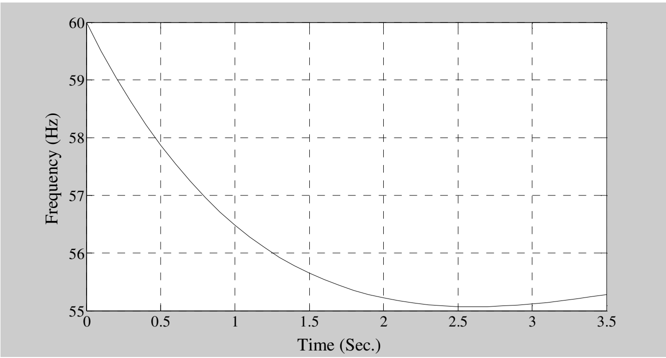

Fig. 1. Lumped system frequency-time response to island conditions for the system in [2] with a generation outage of 0.6 p.u.

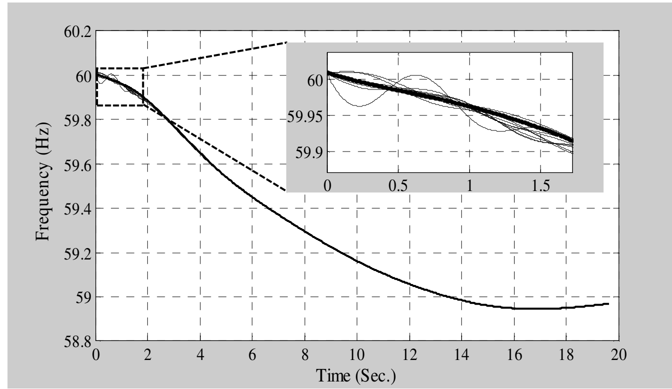

Fig. 2. Generator frequency behavior for the IEEE 39 bus system for an outage of Generator 2 (The COI frequency is shown as the bold center line)

C. *Effect of inter-generation swings on the COI df/dt*

The p.u. COI df/dt is defined as follows:

$$\frac{d\bar{f}_{COI}}{dt} = \left(\sum_{i=1}^{ng} H_i \frac{d\bar{f}_i}{dt} \right) / \sum_{i=1}^{ng} H_i \qquad (2)$$

Where ng = no of generators, H_i = inertia constant of generator i

$\frac{d\bar{f}_i}{dt}$ = p.u. rate of change measured by the PMU at the bus of generator i

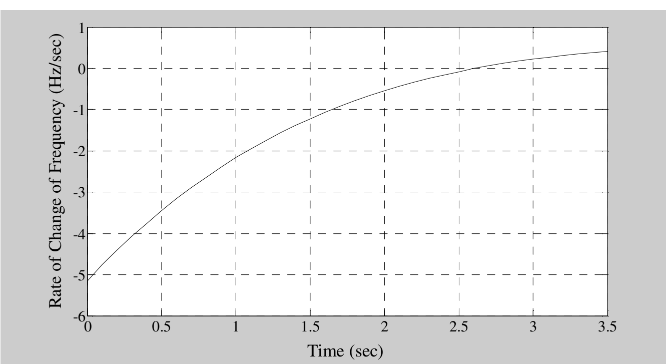

Fig. 3. Typical lumped system rate of change of frequency in response to island conditions for the system in [2] with a generation outage of 0.6 p.u.

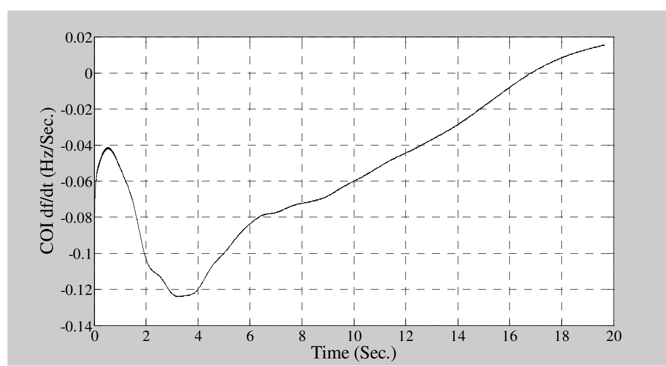

Fig. 4. Rate of change of COI frequency for the IEEE 39 bus system for an outage of Generator 2

The COI df/dt, similar to the COI frequency representation of collective frequency, is typically considered representative of collective system acceleration. It is important however to point out the differences that exist between a lumped and an actual system. Fig. 3 illustrates that lumped system acceleration follows a smooth pattern towards a steady state for a stable system. However, actual COI df/dt for a realistic is more complex; involving initial oscillations related to inter-generator swing behavior and control system dynamics. This is depicted in Fig. 4, which shows the COI df/dt behavior for an outage of Generator 2 on the IEEE 39 bus system.

III. Description of Frequency Prediction Method

A. *Correcting the COI df/dt*

In addition to frequency time-stamped measurements, PMU's also send rate-of-change of frequency measurements to a central synchro-phasor vector processor. The COI df/dt can trivially be obtained in the same way as for COI frequency. The COI df/dt is proportional to the disturbance power which fluctuates due to inter-generator oscillations and system control dynamics. These fluctuations should be removed in pursuit of a system which can be approximated with the linear lumped behavior described by (1). Two methods for smoothing out the unwanted oscillations are presented here; an averaging method and a disturbance power correction method. In both methods, the corrected COI df/dt behavior is estimated in the first few seconds following the disturbance and then that behavior is examined to determine whether or not the system will recover, and if so what are the expected frequency excursions.

B. Smoothing (averaging) of the COI df/dt

The first procedure adopted here is to smooth out the COI df/dt oscillations using a moving-window averaging procedure. The raw df/dt data arriving from the system PMUs is subjected to a progressive averaging process. The simplest form is to simply predefine an averaging span and to reduce the data by taking the average over that span. As new data becomes available from the PMUs the averaging span moves forward. In essence it is a low pass filter removing higher order dynamics. The time span selection is the key to successfully filter unwanted frequencies. This time span depends really on the inter-generation oscillatory characteristics of each individual system and the for the IEEE 39 bus system the period for these frequencies was in the 1.0 second range. An averaging interval of 2.0 s with a 2nd degree polynomial approximation was subsequently used for the study cases attempted here. Fig. 5 shows actual and smoothed COI df/dt against time for the first 5 seconds following an outage event of Generator 2 on the IEEE 39 bus system.

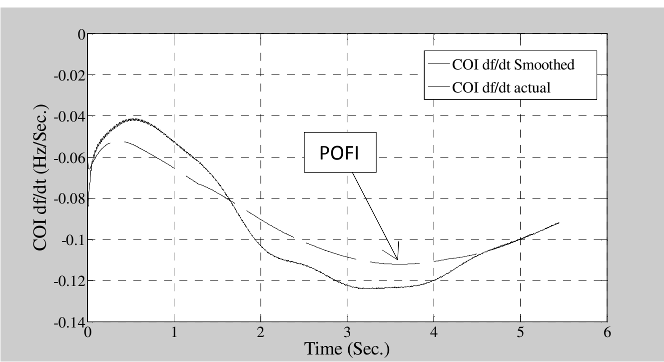

Fig. 5. Actual and smoothed COI rate of change of frequency

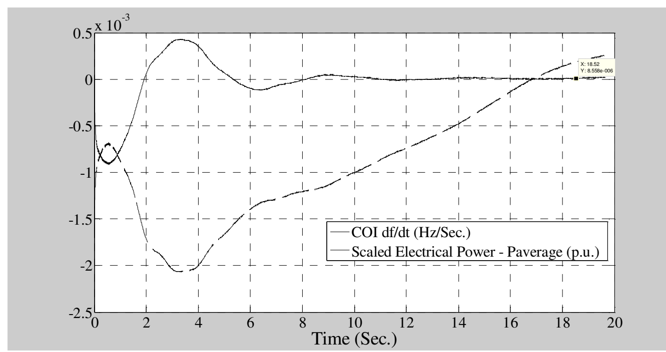

Fig. 6. Total scaled electrical power around average compared with COI df/dt

C. Correction of COI df/dt using disturbance power.

The total p.u. disturbance power is the sum of the individual power mismatches, viz

$$\Delta\overline{P} = \sum_{i=1}^{ng}\left(\overline{P}_{mi} - \overline{P}_{ei}\right) \qquad (3)$$

The disturbance power is related to the p.u. COI df/dt as follows (as long as the frequency deviations in relation to nominal frequency remain small).

$$2H_o \frac{d\bar{f}_{COI}}{dt} = \Delta\overline{P} \qquad (4) \qquad \text{Where } H_o = \sum_{i=1}^{ng} H_i$$

Now the electrical power $\overline{P}_{ei}$ remains constant in a lumped system representation, whereas it fluctuates for actual systems due to inter-generation swings and to system dynamics. If it is possible to obtain the average of these fluctuations over a defined period, then (4) may be rewritten as follows;

$$2H_o \frac{d\bar{f}_{COI}}{dt} = \sum_{i=1}^{ng}\left(\overline{P}_{mi}\right) - \overline{P}_{av} - \sum_{i=1}^{ng}\left(\overline{P}_{ei}\right) + \overline{P}_{av} \qquad (5)$$

The correction term applied to the COI df/dt for the purpose of eliminating inter-generator oscillations is then incorporated as follows;

$$\frac{d\bar{f}_{COI}}{dt} + \frac{1}{2H_o}\left[\sum_{i=1}^{ng}\left(\overline{P}_{ei}\right) - \overline{P}_{av}\right] = \frac{1}{2H_0}\left[\sum_{i=1}^{ng}\left(\overline{P}_{mi}\right) - \overline{P}_{av}\right] \qquad (6)$$

To implement the above correction, the electrical power needs to be collected and averaged. Electrical power from the individual generators is readily available from the PMUs along with frequency data. Fig. 6 shows the total electrical power minus the average power scaled by dividing it with $2H_0$ (the second term on the left hand side of (6) for an outage of Generator 2. On the same figure the COI df/dt is shown to illustrate how closely the two quantities are related.

The quantity P_{av} needs to be estimated. It is not immediately available from the PMU data, but can be found by observing the center of oscillation of electrical power. It is clear that the electrical power behavior closely resembles an exponentially damped sinusoid system and can therefore be modeled using the same expression of (1). To be used in the frequency prediction process the parameters of the expression will have to be estimated in the first few seconds following the disturbance. The second step after the modeling the electrical behavior is to filter out oscillatory behavior. This is done here by eliminating the sinusoid, in effect reducing the model to a first order exponential system of the form

$$P_{av}(t) = \alpha\left(1 + \beta e^{-\gamma t}\right) \qquad (7)$$

This may not be an ideal filtering method, but it is sufficient for our purposes. Fig. 7 shows a plot of actual total electrical power along with estimated power using the first five seconds of data and reduced average electrical power for an outage of generator 2 on the IEEE 39 bus system.

D. Frequency excursion prediction based on smoothed or corrected data.

After smoothing or correcting the COI df/dt it is integrated to regenerate smoothed COI frequency behavior. This replaces the actual COI frequency received from captured real-time measurements by the PMU's. Both smoothed COI frequency and smoothed or corrected COI df/dt are then sampled at regular frequency intervals - spaced in this study at 0.025 Hz intervals – and used to estimate the full frequency excursion range and time to maximum by employing curve fitting analysis. The spacing of 0.025 Hz is not entirely arbitrary and is chosen here to give enough time resolution for parameter estimation. Parameter estimation only starts when the smoothed COI df/dt exhibits signs of system recovery, by showing a consistent trend of increasing values. A frequency sampling resolution of 0.025 Hz will allow four samples for every drop of 0.1 Hz and these samples can then be checked to determine if the system is on its path towards recovery. The authors have also experimented with 0.05 Hz spacing and it gave good predictions but naturally required more time to check for the COI df/dt trend. It is to be noted that if the frequency declines too fast then enough time will not be available to carry out the prediction process and the conventional load shedding scheme would then proceed as normal, as it should.

The parameter estimation itself is a curve fitting exercise for the model described with (1) and is based on a nonlinear least-squares algorithm, specifically the Levenberg-Marquardt method available in Matlab.

E. Implementation of the prediction in real time

The decision to start prediction is based on observing the smoothed or the corrected COI df/dt curve. First a reversal in trend from a negative slope to a positive slope must be observed. This is marked by point POFI (point of frequency inflection) in Fig. 5. Second, after ensuring that a consistently monotonic positive slope ensues, the prediction cycle may begin. If the curve fitting is is successful in finding a solution, then sufficient data has been captured. If it is not then additional real time data is required. The minimum frequency and time to minimum is easily found from (1) as

$$t_{\min} = \frac{\tan^{-1}(\frac{\omega_d}{\varsigma\omega_n}) + \pi - \phi}{\omega_d} \quad (8)$$

$$f_{\min} = f_0 - \Delta f(t_{\min}) \quad (9)$$

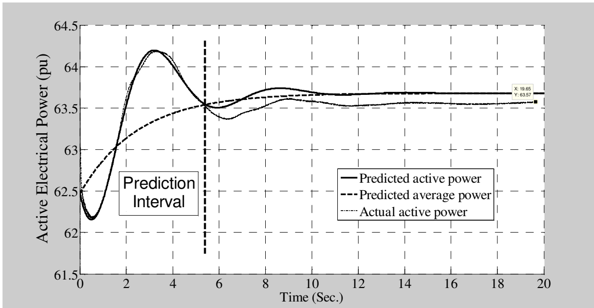

Fig. 7. Actual and estimated active electrical power and estimated COI frequency

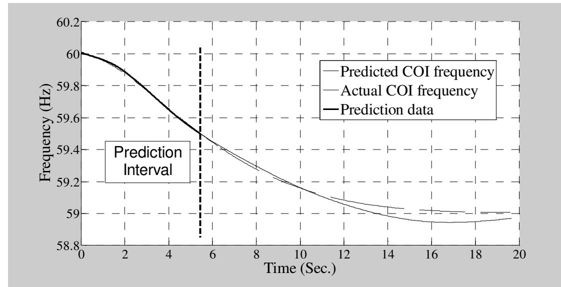

Fig. 8. Actual and predicted COI frequency

IV. Simulation and System Setup

A. Setup Description

The IEEE 39 bus system was simulated in real time using the OPAL_RT real time simulator. Hardware in the loop consisted of PMU relays interfaced to the simulator in addition to a synchrophasor vector processor (SVP) interfaced to both the relays and the computer used for real time prediction.

The test system is shown in the appendix, Fig A1. The Real Time Digital Simulator enables the power system model to interact with the actual hardware in real time. The voltage/current amplifiers connect the simulator to the PMUs and Relays. The PMUs gather synchronized real-time measurements from multiple remote locations on the power system modeled in the simulator and send it to the SVP. The SVP which serves as a central location processes the data received from the PMUs. A GPS clock provides the time reference for PMU's operation.

It is possible to extend this setup to include relays for the purpose of load shedding in case the frequency prediction proves unfavorable for system stability or if the frequency drops too quickly to afford enough time for prediction calculations.

V. Simulation Results and Discussion

A. Study cases

A number of cases were simulated to create island conditions for the IEEE 39 bus system with a total load of 6500 MW. The first case, a loss of generator 2 (386 MW) has already been used as a showcase in the preceding sections illustrating the COI df/dt smoothing and correction and the active power estimation. Upon smoothing the COI df/dt it was possible to locate the point of frequency inflection (POFI) after about 3.6 s. To locate this point and ensure the consistent recovery behavior of the system it was necessary to capture about 5.4 s of data. Smoothing and rebuilding the COI frequency took about 0.018 s of CPU time on a general purpose computer running Windows, while the least-square estimation and prediction required 0.21 s. Overall the prediction window required 5.6 to capture enough data and to perform the analysis, predicting the minimum frequency at 59.01 Hz after 20.26 s from the start of the event. The actual minimum frequency of the simulation was 58.95 Hz after a time of 16.83. Fig. 8 shows the actual and predicted COI frequency for this event. The prediction interval is also shown and indicates that a prediction is available by the time the frequency has dropped to 59.5 Hz.

The second method which involved correction of the COI df/dt instead of smoothing yielded a minimum frequency of 59.01. This was very similar to the first method but the prediction was somewhat overdamped and gave a time to minimum frequency of 23.71 s. This approach required slightly more time than the smoothing method and took about 5.7 s to yield a prediction.

Additional cases were simulated comprising outages on generators 5, 6, 9 and 10. Table 1.0 summarizes the actual minimum frequency excursion and time to minimum along with the predictions of the same using both methods.

TABLE I
Summary of Frequency Predictions

Gen outage	Outage MW	Actual Simulation		Method 1 (Smoothing)		Method 2 (Correcting)	
		F_{min} (Hz)	T_{min} (Sec.)	F_{min} (Hz)	T_{min} (Sec.)	F_{min} (Hz)	T_{min} (Sec.)
G2	386	58.95	16.83	59.01	20.26	59.01	23.72
G5	500	58.53	16.50	58.79	13.4	58.62	31.12
G6	650	57.95	17.42	58.22	15.37	57.99	29.39
G10	370	59.09	16.01	59.26	18.33	59.11	27.67
G9	830	57.28	16.56	No Prediction			

B. Discussion

Two cases are particularly of interest. The first is an outage on generator 6 (650 MWs) and causes the frequency to drop to 59.95 Hz. The second method predicts a frequency drop of 57.99 Hz. Since NERC requirement 3 [3] states that the system frequency must be above 58 Hz this event represents a case where load shedding should not be withheld and should be allowed to proceed to comply with the criteria. The second case of interest is an outage on generator 9 (830 MWs). Because of the large area imbalance the frequency drops rapidly and crosses to below 59 Hz in less than 4.3 s, and this occurs before the smoothed COI df/dt shows signs of a definite reversal of trend towards recovery. This time slot is too short to perform a prediction and it is not advisable to withhold shedding until such a prediction becomes available.

Overall both methods were able to predict the frequency with a fair margin of error; the second method offered excellent frequency prediction with a maximum error of 0.15% but performed rather poorly in time-to-minimum estimation which in some cases rose to 88% over the actual time. The first method had a maximum frequency prediction error of 0.46% and its time-to-minimum estimation was much better, only exceeding by 20% for the worst case.

The second method relies on correction of COI df/dt by removing inter-generation oscillations. Excessive removal of oscillatory behavior may lead to overdamping in the predicted frequency, since not all oscillatory behavior is unwanted, and it is important to retain information that is related to collective system dynamics. The key to this lies in the method used to average the electrical power, which in this study is an order reduction from a second to a first-order system. The time delays associated with the second method are clear indications of overdamping and it would be perhaps productive to experiment with a method of averaging that better preserves collective acceleration information.

Having noted the above, it is to be pointed out that the time-to-minimum is not as critical a constraint as the minimum frequency itself. The NERC document gives about 60 s of operation between 58 Hz and 58.8 HZ in an inverse frequency-time relationship, and this provides ample time to monitor the frequency and to initiate shedding if frequency stalls at a value violating the required frequency performance characteristics mandated by the standard. It is also pointed out that this time-to-minimum tends to be almost constant and fairly independent of the size of the disturbance. In this study it was in the range of 16 – 17 s for the cases examined and hence could be expected to remain the same for most outages.

The essence of the methods laid out in this study is to monitor the rate of change of frequency to assess system recovery. This is not a new idea and has been discussed before, for example in [7]. However it was not used for frequency prediction; only as a tool to aid and optimize load shedding.

Furthermore most discussions hitherto on using COI df/dt involved waiting for the inter-generation oscillation transients to subside before any meaningful trend could be inferred from it. In this study, such a delay would be unacceptable as the objective is to avoid load shedding if possible and thus useful information must be extracted from the COI df/dt from the very beginning and while it is distorted by inter-generator dynamics and other influences. Both smoothing the COI df/dt and correcting it using the electrical power gave excellent results in terms of minimum frequency prediction, with the second method being superior in this regard.

VI. CONCLUSIONS

A method for real-time minimum COI frequency prediction in the event of an islanding condition was presented. The method relies on captured data from PMUs at the generator locations which essentially comprises individual generator frequencies and df/dt. The method is further enhanced if the electrical power generation is also received from the same PMUs. Collective system behavior is discerned from the data by applying smoothing or correction actions on the COI df/dt. The smoothed or corrected COI df/dt is then monitored until its trend reflects consistent system recovery. Minimum frequency and time-to-minimum is then predicted, if the time span required for data capture, analysis and prediction is available before the frequency drops excessively to below 59 Hz as suggested in this study. If prediction is not possible load shedding is to be commenced as usual. Otherwise utilities may use this centralized approach to withhold shedding and subsequently monitor the recovery trend. The prediction of minimum frequency using either the smoothing or correction approach was found to be of good accuracy, while the time-to-minimum exhibited signs of over-damping in the prediction, particularly for the second approach. The authors would recommend further investigation on this by searching for an improved method of averaging the electrical power while retaining bulk oscillation.

It is hoped that the idea that load-shedding need not be initiated upon violation of certain frequency thresholds will find some attraction among utilities and regional reliability corporations in the interest of averting unnecessary interruptions to the customers as long as this “wait-and-see” approach is deemed satisfactorily in compliance with NERC regulations.

BIBLIOGRAPHY

[1] S. AbdElwahid, A. Babiker, A. Eltom and G. Kobet, "Hardware Implementation of an Automatic Adaptive Centralized Underfrequency Load Shedding Scheme" (IEEE transactions on Power Delivery, vol. 29, no. 6, 2014 pages 2664-2673)

[2] P. Anderson and M. Mirheydar, "An Adaptive Method for Setting Underfrequency Load Shedding Relays" (IEEE Transactions on Power Systems, vol. 7, no. 2, May 1992, pages 647-655)

[3] NERC Reliability Standard PRC-006-1-Automatic Underfrequency Load Shedding, NERC (October 1, 2013), available at (http://www.nerc.com/files/prc-006-1.pdf).

[4] Maria Vrakopoulou, Göran Andersson, "An Adaptive Load Shedding Technique for Controlled Islanding,” Power Systems Computation Conference (PSCC), Stockholm, Sweden, 2011.

[5] IEEE Power Systems Test Case Archive. Available from: (https://www.ee.washington.edu/research/pstca/)

[6] Anderson, P.M. and Mirheydar, M. "A low-order system frequency response model," (IEEE Transactions on Power Systems, vol 5, no. 3, 1990, pages 720-729).

[7] U. Rudez and R. Mihalic, "Monitoring the First Frequency Derivative to Improve Adaptive Underfrequency Load Shedding Schemes" (IEEE transactions on Power Systems, vol. 26, no. 2, May 2011, pages 839-846).

APPENDIX

Figure A1 shows the system setup for IEEE 39 bus real-time digital simulation with PMU and SVP hardware.

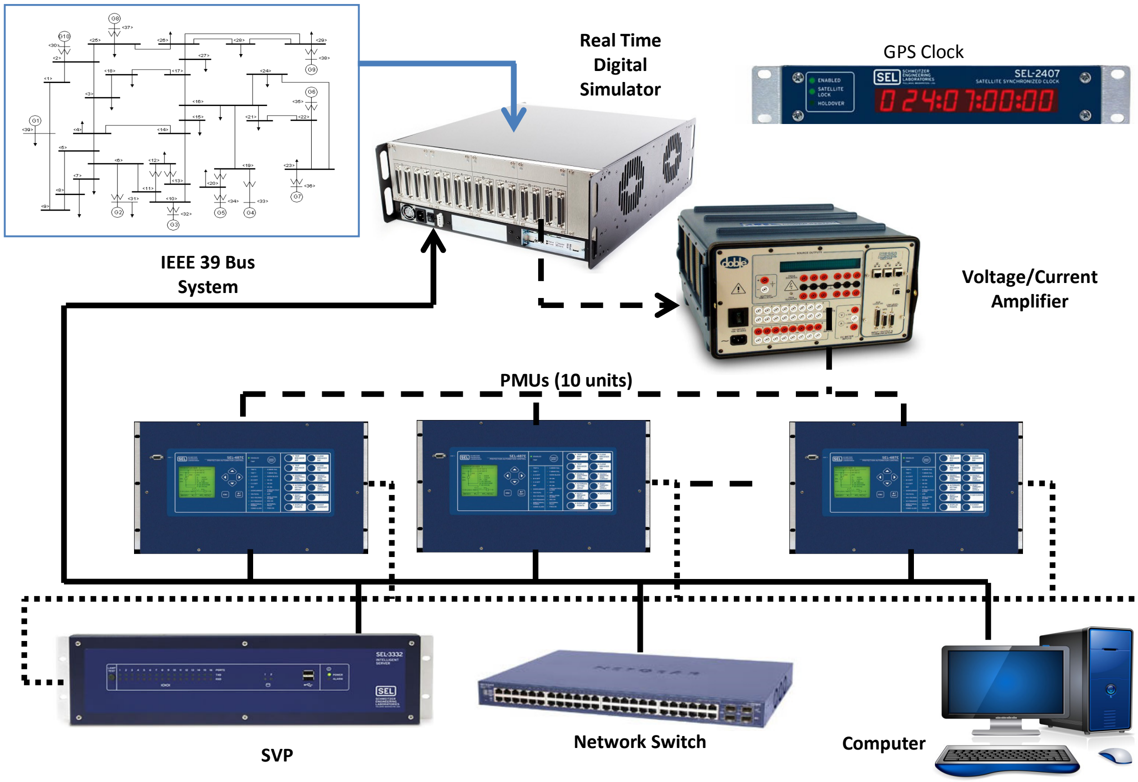

Fig. A1. Test system setup.